Longitudinal and Temporal Evolution of the Tectonic Style Along the Cyprus Arc System, Assessed Through 2-D Reflection Seismic Interpretation

Vasilis Symeou, Catherine Homberg, Fadi H. Nader, Romain Darnault, Jean-claude Lecomte, Nikolaos Papadimitriou

Longitudinal and Temporal Evolution of the Tectonic Style Along the Cyprus Arc System, Assessed Through 2-D Reflection Seismic Interpretation

Vasilis Symeou[1,2], Catherine Homberg[1], Fadi H. Nader[2], Romain Darnault[2], Jean-Claude Lecomte[2], and Nikolaos Papadimitriou[1,2]

[1]ISTEP, Universite Pierre et Marie Curie, Paris, France, [2]Geosciences Division, IFP Energies nouvelles, Rueil-Malmaison, France

Key Points:
- Lateral changes from a compressional to a strike-slip regime along the Cyprus Arc
- Different crustal nature in the eastern Mediterranean
- Forward propagation of thrusting toward the south

Correspondence to:
V. Symeou,
symeouvas@gmail.com

Citation:
Symeou, V., Homberg, C., Nader, F. H., Darnault, R., Lecomte, J.-C., & Papadimitriou, N. (2018). Longitudinal and temporal evolution of the tectonic style along the Cyprus Arc system, assessed through 2-D reflection seismic interpretation. *Tectonics*, *37*. https://doi.org/10.1002/2017TC004667

Abstract The Cyprus Arc system constitutes a major active plate boundary in the eastern Mediterranean region. This structure is directly linked with the northward convergence of the African and Eurasian plates since the Late Cretaceous. Two-dimensional reflection seismic data were utilized, which image the main plate structures and their lateral evolution south of the island of Cyprus. Interpretation of these data allowed the identification of nine tectono-sedimentary packages in three different crustal domains south of the Cyprus Arc system: (1) the Levant Basin (attenuated continental crust), (2) the Eratosthenes microcontinent (continental crust), and (3) the Herodotus Basin (oceanic crust). Within these domains, numerous tectonic structures were documented and analyzed in order to understand the mechanism and timing of deformation. In the north, south verging thrusting commenced in early Miocene along the Larnaca and Margat ridges, whereas no activity was identified before middle Miocene along the Latakia Ridge. Thus, the deformation front migrated southward and was accompanied by the development of flexural basins and stratigraphic onlaps as in the Cyprus Basin. The acme of deformation occurred in mid-late Miocene. A regional unconformity of Pliocene age marks the end of the first deformation sequence. In Plio-Pleistocene time, the westward escape of the Anatolian microplate resulted in the reactivation of existing structures. The evolution of deformation along the plate boundary is identified from the creation of positive flower structures revealing transpressive movements along the Larnaca and Latakia Ridges (eastern domains), whereas in the Eratosthenes domain a flexural basin highlights a compressive regime.

Plain Language Summary The Cyprus Arc system is situated at the boundary of the Arabian, African, and Eurasian plates and is associated with a convergent setting, which is active since the Late Cretaceous, in response to the northward movement of the African plate with respect to the Eurasian plate. Two-dimensional seismic interpretation resulted in the identification of different crustal domains, which are the following: (1) the Levant Basin, (2) the Cyprus Basin, (3) the Eratosthenes Seamount, and (4) the Herodotus basin. These domains are underlain by a different crustal nature and record contractional pulses from Neogene to Recent time. Thrusting activity is dominant in Miocene time on the Latakia, Margat, and Larnaca Ridges, with the deformation style best described by a forward propagation model. In Plio-Pleistocene time a strike-slip component is observed, which is associated with the westward escape of the Anatolian microplate. In this contribution the longitudinal evolution along the Cyprus Arc is presented in relation with the differential crustal nature of each domain.

1. Introduction

The geological evolution of the eastern Mediterranean, which is directly linked with the opening and closing of the Neo-Tethys ocean (Gardosh et al., 2010; Garfunkel, 1998, 2004; Stampfli & Borel, 2002), has attracted great interest and is still debated. The Cyprus Arc system, which includes the Cyprus Island, is located in the central part of the eastern Mediterranean region and constitutes the present-day boundary of the African and Anatolian plates (Figure 1).

Different scenarios attempting to describe the tectonic evolution of the region exist. The three main scenarios are the following: (a) long-lived collision scenario: depicting continuous thrusting and folding onshore and offshore Cyprus from Eocene until recent as a result of the continent-continent collision between the African and Eurasian plates. This scenario is suggested by the change in facies of the juxtaposed Paleogene-Oligocene deep pelagic carbonates with the Miocene flysch deposits in the Mesaoria basin, a

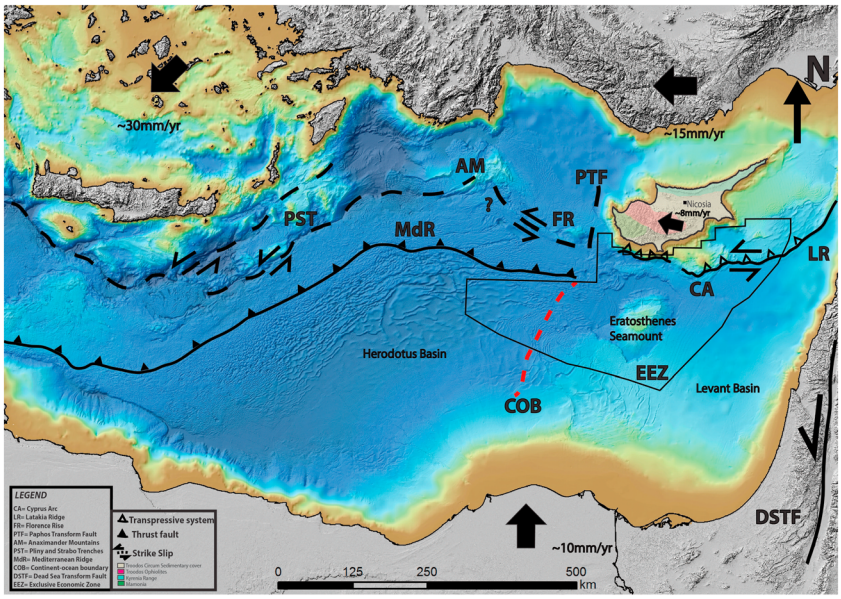

Figure 1. Regional bathymetric map (*EMODnet*), with the main tectonic structures. The red dashed line delineates the boundary between the thin continental crust (Levant Basin) and the oceanic crust (Herodotus Basin) as it was identified by Granot (2016). The black arrows indicate the relative motion and average slip rate for the African and Anatolian plates (McClusky et al., 2000). *Abbreviations:* AM = Anaximander Mountain, CA = Cyprus Arc, COB = Continent-ocean boundary, DSTF = Dead Sea Transform Fault, EEZ = Exclusive Economic Zone of Cyprus, FR = Florence Rise, HA = Hellenic Arc, LR = Latakia Ridge, MdR = Mediterranean Ridge, PTF=Paphos Transform Fault, PST = Pliny and Strabo Trenches.

basin considered as a piggyback basin which developed between the Troodos-Larnaca culmination and the Kyrenia thrust belt (Calon et al., 2005a, 2005b; Sage & Letouzey, 1990); (b) strike-slip scenario, supported by the absence of a volcanic arc and a Benioff zone offshore Cyprus, in addition to the recognition of strike-slip structures onshore, which suggests that the emplacement of the ophiolites and the creation of the Cenozoic basins and Recent structures are associated with a left-lateral strike-slip regime since Late Cretaceous (Harrison, 2008; Harrison et al., 2012); and (c) Pliocene collision scenario: where the Pliocene compressional tectonics followed a succession of compressional (from Late Cretaceous to Paleogene) and extensional regimes (Miocene time due to slab roll-back of the northward subducting African plate). This last scenario rests on the recent uplift of Cyprus and the change in sedimentation from Miocene hemi-pelagic carbonates to Pliocene clastics as a result of the continent-continent collision between the Eratosthenes microcontinent and the Eurasian plate in Pliocene (Kempler, 1998; Kinnaird et al., 2011; Robertson, 1998; Robertson et al., 2012).

These different models/scenarios highlight the main plate-scale driving mechanisms responsible for the Cenozoic deformations in the eastern Mediterranean region. The deformation commenced with the northward convergence of the Afro-Arabian plates with respect to Eurasia and is later accompanied by the westward extrusion of the Anatolian microplate relative to the African plate through time. Only a limited amount of published work on the Cyprus Arc system focuses on the lateral evolution of the structural style along this major boundary. Even less emphasis is given on the integration of the tectonic structures of the Cyprus Arc system within the frame of the complex nature of the eastern Mediterranean basin.

Recent magnetic and gravity studies (Granot, 2016) indicate the boundary between the thinned stretched continental crust of the Levant Basin (Granot, 2016; Inati et al., 2016; Montadert et al., 2014; Netzeband et al., 2006) and the oceanic crust of the Herodotus Basin (Granot, 2016; Montadert et al., 2014) (Figure 1, red dashed line). This entices us to investigate the following scientific interrogations: How is the convergent movement of the plates and the deformation along the Cyprus Arc accommodated in this type of setting? Does the variation of the crustal nature affect the deformation style?

The main objective of this paper consists in investigating the aforementioned questions related to the structural style of deformation and the crustal variation between the eastern, central, and western domains. In the

eastern domain thin continental crust (Levant Basin) and obducted ophiolite (Cyprus Basin) are in contact. In the central domain the continental crust underneath the Eratosthenes microcontinent is colliding with the continental crust under Cyprus. Finally in the western domain, the oceanic crust of the Herodotus Basin is subducting northward under the continental crust of the Antalya Basin (southern margin of Turkey). Interpretation of industrial quality 2-D (two-way travel time (TWTT)) seismic reflection data, which cover the Exclusive Economic Zone offshore Cyprus (Figures 1 and 3), was the key tool utilized in order to materialize this objective. These seismic data cover the E-W extension of the Cyprus Arc system, which allows for comparison with previous data in order to observe along strike the lateral evolution of the Arc system, by mapping the various tectonic structures in order to deduce the mechanism and timing of the observed deformations.

2. Geological Setting

The tectonic evolution of the eastern Mediterranean starts with the breakup of the supercontinent of Pangea and the creation of the Neo-Tethys Ocean (Frizon de Lamotte et al., 2011; Gardosh et al., 2010). Rifting was followed by a convergent phase, resulting in the creation of tectonic structures (i.e., Cyprus Arc system), and the emplacement of the ophiolitic belt (Garfunkel, 1998) from East in Baer-Bassit in Syria, through Troodos Mountains in Cyprus to the West in the Antalya region in Turkey.

2.1. Early Triassic-Early Cretaceous

The Early Mesozoic period is considered as the onset of fragmentation of the northern margin of the supercontinent of Pangea and the beginning of Tethys rifting (Gardosh et al., 2010; Montadert et al., 2014). This breakup resulted in the creation of smaller continental fragments, such as the Tauride microcontinent, which drifted northward from the northern margin of Gondwana toward the Eurasian plate (Bowman, 2011; Garfunkel, 2004). The outcome was the opening of the Neo-Tethys Ocean in late Middle Jurassic time (Callovian time) (Barrier & Vrielynch, 2008; Frizon de Lamotte et al., 2011) and the gradual creation of smaller oceanic basins, separated by the resulting continental fragments (Robertson, 2007; Robertson et al., 2012). Rifting commenced in Mid-Triassic (Anisian) and halted in Mid-Late Jurassic time (Bowman, 2011; Gardosh et al., 2010; Gardosh & Druckman, 2006; Montadert et al., 2014). Tethys rifting (Figure 2, box A) culminated in the creation of the Levant Basin from an extensional regime oriented in a NW-SE direction, with NE-SW trending normal faults (Gardosh et al., 2010; Gardosh & Druckman, 2006; Garfunkel, 1998). The Levant Basin is regarded as a basin overlain by ~12–14 km of sediments of probably Triassic-Jurassic age until recent (Ben-Avraham et al., 2002; Makris et al., 1983; Montadert et al., 2014; Vidal, Alvarez-Marron, & Klaeschen, 2000; Vidal, Klaeschen, Kopf, Docherty, Von Huene, & Krasheninnikov, 2000), with its crustal nature considered as a thin attenuated continental crust of ~8 km (Granot, 2016; Inati et al., 2016; Netzeband et al., 2006; Segev et al., 2011). In contrast, the Herodotus Basin is constructed of oceanic crust (Granot, 2016; Makris et al., 1983) and is covered by a thick sedimentary sequence of ~14–16 km (Montadert et al., 2014). Ongoing rifting (Gardosh & Druckman, 2006) resulted in the "separation" of the Eratosthenes microcontinent from the Arabian continental plate (Montadert et al., 2014). Faulting ceased by Mid-Late Jurassic time in the southern Levant, whereas tectonic activity continued during Early Cretaceous onshore Lebanon (Homberg et al., 2010).

2.2. Upper Cretaceous-Oligocene

The Upper Cretaceous period is regarded as the start of the convergence regime between the African and Eurasian plates (Bowman, 2011; Gardosh et al., 2010; Klimke & Ehrhardt, 2014; Montadert et al., 2014) and the inversion of the eastern Mediterranean basins. In Late Maastrichtian, the initial closing stage of the Neo-Tethys Ocean results in the obduction of ophiolites in Baer-Bassit-Syria, in Antalya-Turkey, and in Troodos-Cyprus (Garfunkel, 2004) (Figure 2, box B) described as the peri-Arabian ophiolitic crescent that extends from Turkey and Cyprus to the Oman ophiolites (Ricou, 1971). Some authors suggest that the Latakia Ridge system initiated during Late Cretaceous time, as a compressional fold-thrust belt due to the convergent movement between the African and Eurasian plates (Bowman, 2011; Vidal, Alvarez-Marron, et al., 2000; Vidal, Klaeschen, et al., 2000). In late Eocene to early Oligocene time the ongoing convergence of the African and Eurasian plates led to the closure of the eastern strand of the Neo-Tethys Ocean (Barrier & Vrielynch, 2008; Bowman, 2011; Frizon de Lamotte et al., 2011).

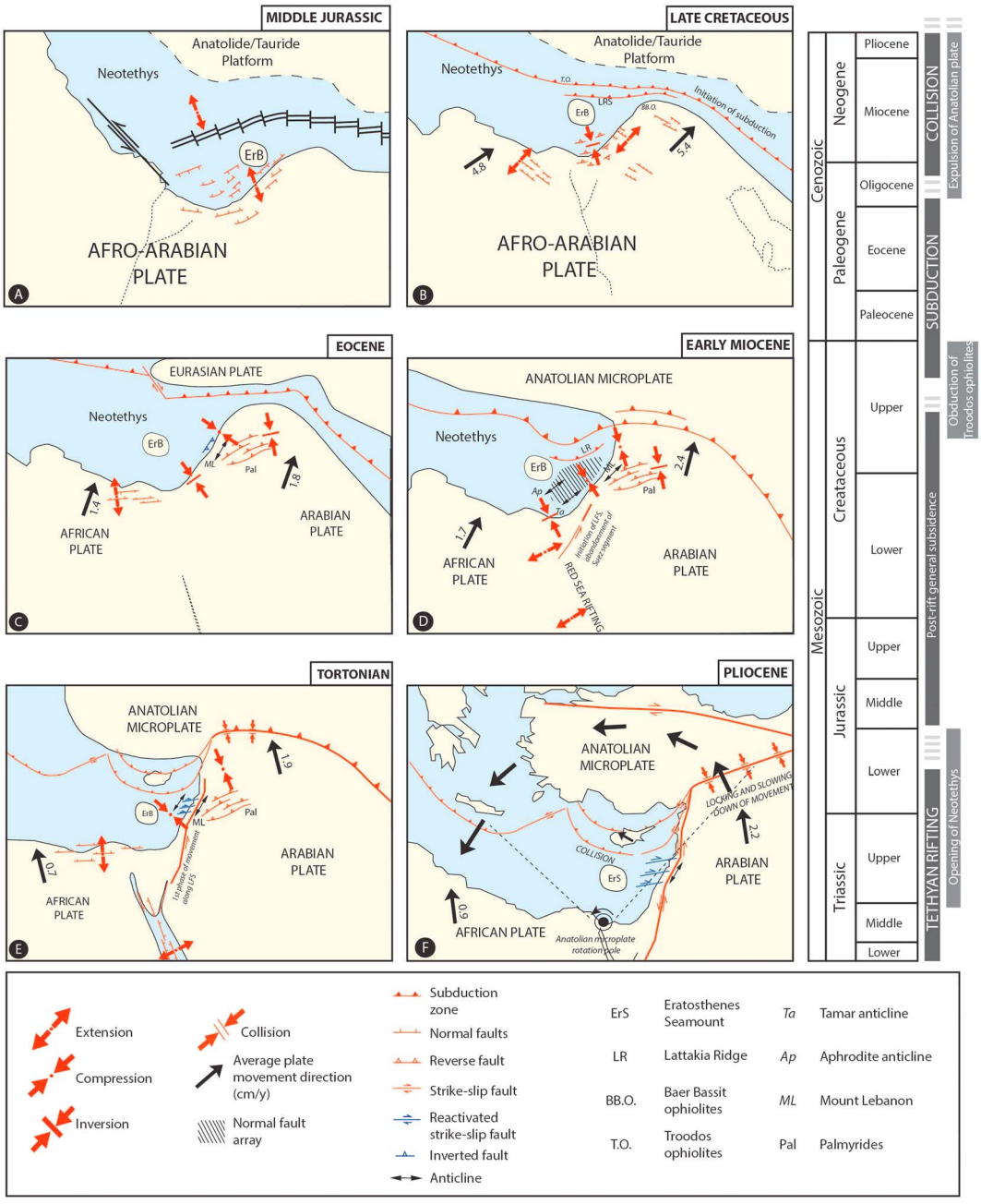

Figure 2. Paleo-geographic maps of the Levant region illustrating the tectonic evolution: (a) Mesozoic rifting phase, normal fault activity ceases by Middle Jurassic time; (b and c) initial closure of the Neo-Tethys due to convergence; (d) initial folding along the Levant margin; (e) westward expulsion of the Anatolian microplate; and (f) current tectonic regime (modified from Ghalayini et al., 2017).

2.3. Miocene–Present

By Miocene time, the "separation" between Arabia and Africa resulted in the initiation of the Dead Sea Transform fault (Montadert et al., 2014). This event was largely due to the difference in motion between the two plates. The increased northward movement of Arabia relative to Eurasia (~18–25 mm/yr (McClusky et al., 2000)), in comparison with the smaller movement of the African plate relative to Eurasia (~10 mm/yr; McClusky et al., 2000), was accommodated by the opening of the Red Sea and the propagation of the Dead Sea Transform Fault (Brew et al., 2001).

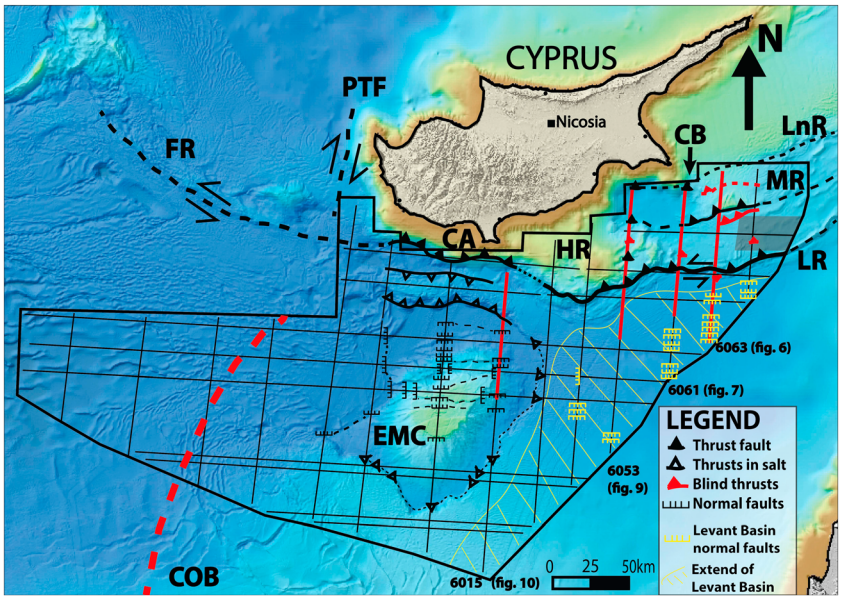

Figure 3. Map of offshore Cyprus. Main structural elements identified after seismic interpretation. The red dotted line delineates the transition boundary between continental and oceanic crust (Granot, 2016). The black thin lines delineate the available seismic data, while the red thick lines delineate the seismic profiles illustrated in this paper. *Abbreviations:* CA = Cyprus Arc, CB = Cyprus Basin, COB = Continent-ocean boundary, ES = Eratosthenes microcontinent, FR = Florence Rise, HR = Hecataeus Rise, LnR = Larnaca Ridge, LR = Latakia Ridge, MR = Margat Ridge, PTF = Paphos Transform Fault.

The westward escape of the Anatolian plate is associated with the slab pull of the northward subducting Hellenic Arc system and the asthenospheric flow (Le Pichon & Kreemer, 2010) in the Aegean region. This slab pull effect is created due to the slab roll back of the subducting Hellenic Arc resulting in an extensional regime and arc volcanism, which is observed in the south Aegean (Dilek & Altunkaynak, 2009; Dilek & Sandvol, 2009) and is correlated quoted as the main mechanism for the escape of the Anatolian plate (Le Pichon & Kreemer, 2010). A second scenario proposes that the western movement of the Anatolian plate is related with the northward movement of the Arabian plate during latest Miocene to early Pliocene time (Hall, Calon, et al., 2005; McClusky et al., 2000, 2003; Montadert et al., 2014).

A consequence of the westward movement of the Anatolian microplate was the creation of a triple junction point, where the East Anatolian fault (left-lateral strike-slip fault), the North Anatolian fault (right-lateral strike-slip fault), and the Dead Sea Transform fault (left-lateral strike-slip fault) meet (Aksu et al., 2005; Kempler & Garfunkel, 1994). In addition, strike-slip faulting in the eastern part of the Cyprus Arc system and the initiation of the strike-slip movement along the Latakia Ridge system occurred at the same time and facilitated Anatolia's escape tectonics (Kempler & Garfunkel, 1994; Montadert et al., 2014).

Bowman (2011), proposes that the initial compressional nature of the Latakia Ridge system changes to a left-lateral strike-slip regime during Pliocene to Recent times, as it is supported by positive flower structures identified from the interpretation of seismic data that cover the Northern part of the Levant Basin and the Cyprus Basin (Bowman, 2011; Hall, Aksu, Calon, & Yasar, 2005; Hall, Calon, Aksu, & Meade, 2005). This change in motion is associated with the reorganization of tectonic stresses of the major plates in the region by late-Miocene to early-Pliocene time (Bowman, 2011), which is in accordance with analogue modeling experiments indicating slab break-off under the Bitlis-Zagros suture zone (Faccenna et al., 2006).

Kinnaird and Robertson (2012) suggest that the ECB collided with the Cyprus Arc during early Pliocene times, thus subducting underneath the arc and causing uplift of the island of Cyprus (Garfunkel, 1998; Robertson et al., 2012). Analysis of plate kinematics and GPS velocities (McClusky et al., 2000, 2003; Reilinger et al., 2006) suggests that the African plate moves toward the N-NW, while the Anatolian plate is experiencing a counterclockwise rotation. These two movements are in accordance with the left-lateral strike-slip movement proposed for the Latakia Ridge (Bowman, 2011; Hall, Aksu, et al., 2005; Hall, Calon, et al., 2005; Le Pichon & Kreemer, 2010; Vidal, Alvarez-Marron, et al., 2000; Vidal, Klaeschen, et al., 2000).

3. Data and Methodology

A multiclient seismic reflection data library courtesy of Petroleum Geo-Services (PGS) exists offshore Cyprus. This database includes 12,200 km of 2-D seismic data shot with the dual sensor GeoStreamer® technology; 6,770 km of conventional 2-D seismic; and 5,000 km^2 of 3-D data covering the Exclusive Economic Zone (EEZ) of Cyprus (Figure 1) (https://www.pgs.com/data-library/europe/mediterranean/). For the purposes of this study and under the authorization of PGS and the Ministry of Energy, Commerce, Industry and Tourism of Cyprus, access to 24 lines of 2-D seismic data was granted (Figure 3).

The conventional 2-D seismic lines were acquired during the MC2D-CYP2006 survey and cover 6,770 km of the EEZ. One conventional hydrophone streamer was used extending 8100 m, with a shot interval of 25 m, a sample rate of 2 ms, and a recorder two-way travel time (TWTT) of 9,216 ms in water depths of 1,000 to 2,500 m. The chosen seismic grid (seismic profile spacing) for this first survey was 10 × 20 km. Ten conventional 2-D seismic lines, reprocessed by PGS in 2011, are available for this project.

With the use of the dual-sensor GeoStreamer® technology, a second survey, MC2D-CYP2008, that covers 12,200 km of the EEZ was acquired in 2008, with the processing completed in 2009. The dual sensor was utilized with a cable length of 8,100 m; a shot interval of 25 m; a sample rate of 2 ms; and a recorder two-way travel time (TWTT) of 9,216 ms in water depths extending from 1,000 to 2,500 m. The gridding for the second survey was 20 × 20 km in the western side, while a denser grid of 5 × 5 km was drawn in the eastern side. Fourteen lines of the second survey are utilized in this project. The use of the dual sensor technology ensured an improved signal-to-noise ratio and better seismic imaging in geological areas with complex structures and a thick salt deposition of 1.5–2 km (Hsu et al., 1977), as subsalt imaging with the conventional methods did not herald good results. Towed at a deeper depth, it ensured a quieter environment and less noise providing a better image (Montadert et al., 2010).

Both data sets were processed by PGS as "conventional marine data including SRME, noise removal in common depth point domain, Kirchhoff prestack time migration, residual moveout correction, radon demultiple, and poststack processing" (see also Montadert et al., 2010).

The seismic data were loaded in GeoFrame Charisma (v. 4.4), a 2-D interpretation software available at IFP Energies nouvelles (Rueil-Malmaison). The identification of different seismic packages and the picking of fault planes from the offset horizons were undertaken through this software. A velocity model provided by PGS was loaded in the GeoFrame Charisma database in order to convert the picked horizons from two-way travel time to depth, allowing for the creation of depth grids.

4. Results

4.1. Seismo-stratigraphy and Structural Domains

Description and interpretation of seismic horizons and seismic packages were composed in accordance with previous studies (Bowman, 2011; Gardosh et al., 2010; Ghalayini et al., 2014; Hawie et al., 2013; Roberts & Peace, 2007) as there is a lack of physical evidence (no access to borehole data) in the investigated area. Eight major seismic packages were identified from the interpretation of the reflection seismic data at our disposal (Figure 3) (courtesy of PGS and the Cyprus Ministry). These packages are constrained by nine key regional horizons (Figure 4) (Bowman, 2011; Gardosh et al., 2010; Hawie et al., 2013; Roberts & Peace, 2007): R9-Seabed, R8-Base Pliocene, R7-Base Messinian, R6-Base mid-Miocene, R5-Top Oligocene, R4-Eocene unconformity, R3-Senonian unconformity, R2-Top Jurassic, and R1-Middle Jurassic.

The R1 is a high-amplitude horizon that delimits the deepest chaotic seismic package identified on the data from a seismic package with more continuous reflectors. Horizon R2 is a high-amplitude continuous horizon that delimits the Upper Jurassic from the overlying Lower Cretaceous seismic unit. The R3 horizon corresponds to a regional unconformity described as the Senonian unconformity and correlates with a major subsidence of the Levant Basin. Horizon R4 represents the Eocene unconformity where lowstand siliciclastic sediments (deposited from the uplift and tilting of the eastern Levant margin) are overlaid by deep marine Oligocene sediments (mixed system of carbonates, shales, and marls), which indicate the continuous subsidence of the Levant Basin. Horizon R5 is the lower boundary of the early Miocene sediments, which are characterized as deepwater clastic deposits. The R6 horizon, of mid-Miocene age, is a high-amplitude reflector identifiable throughout the Levant Basin (Gardosh et al., 2010; Hawie et al., 2013). The R7 horizon is

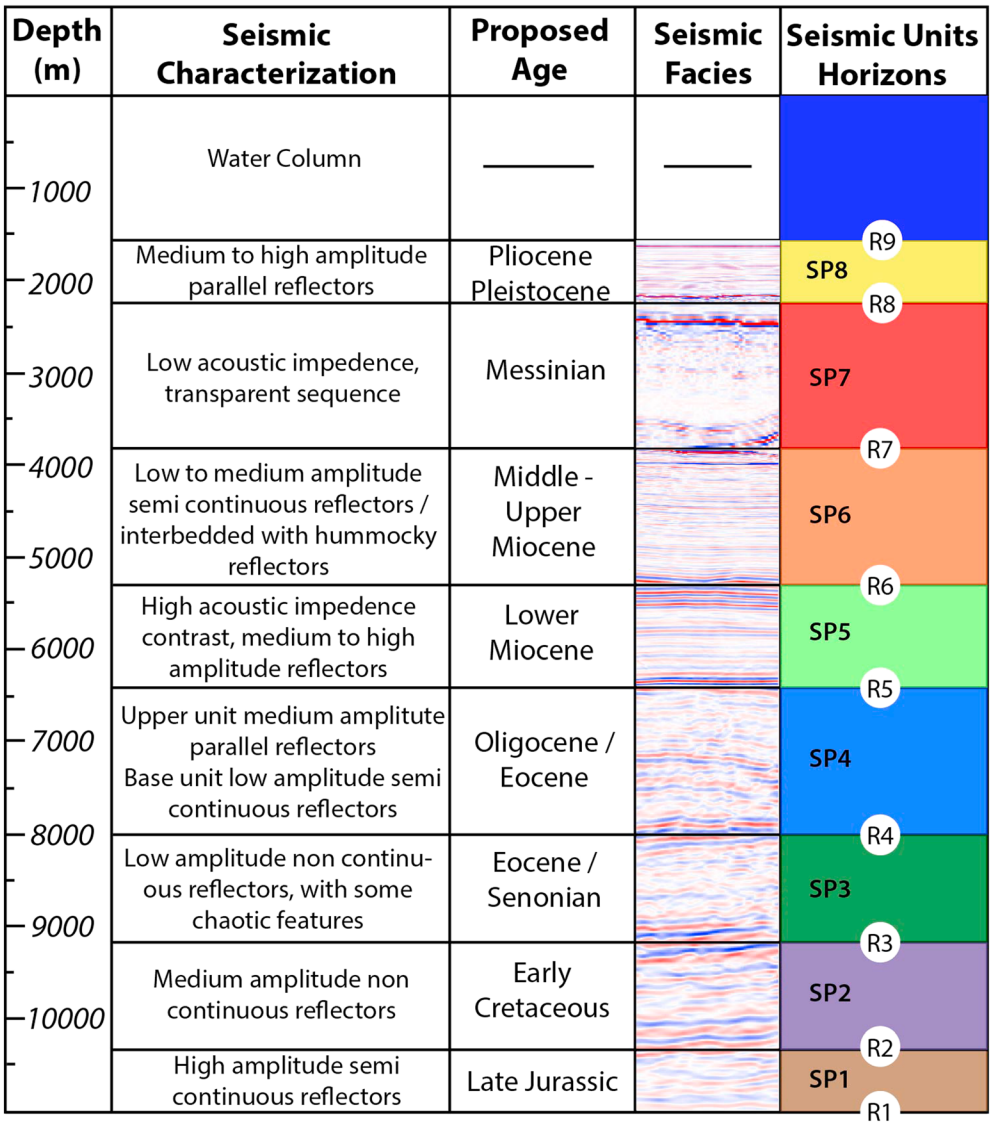

Figure 4. Chrono-stratigraphic chart depicting the horizons identified during seismic interpretation with the proposed ages, seismic facies and thicknesses.

considered as the Base Messinian horizon overlain by the evaporitic sequence, mixed with some lowstand clastics derived from the Nile Delta. Horizon R8 relates to the inundation of the Mediterranean Sea during Pliocene time and the deposition of hemi-pelagic sediments (Hawie et al., 2013). Finally, R9 horizon represents the seabed.

The study area can be subdivided in four different domains, based on the seismic interpretation and the identification of the different horizons and seismic packages (Figure 5). The first domain relates to the Levant Basin (Figure 5a), and it is located south-east of Cyprus (Figure 5, box 5A). The Levant Basin, which is floored by a thin attenuated continental crust (Inati et al., 2016), is infilled by a thick sedimentary sequence of ~12–14 km. This deepening of the basin is directly linked with the continuous subsidence of the Levant Basin and the uplift of the eastern passive margin (Hawie et al., 2013).

The second domain is the Cyprus Basin (Figure 5b) just east of Cyprus (Figure 5, box 5B). It is proposed that this basin is floored by obducted ophiolites and constitutes the continuation of the Troodos ophiolites toward the east where it connects with the Baer-Bassit ophiolites of Syria (Calon et al., 2005a, 2005b; Bowman, 2011). The uplifted position of the Cyprus Basin due to the compressional events in the region

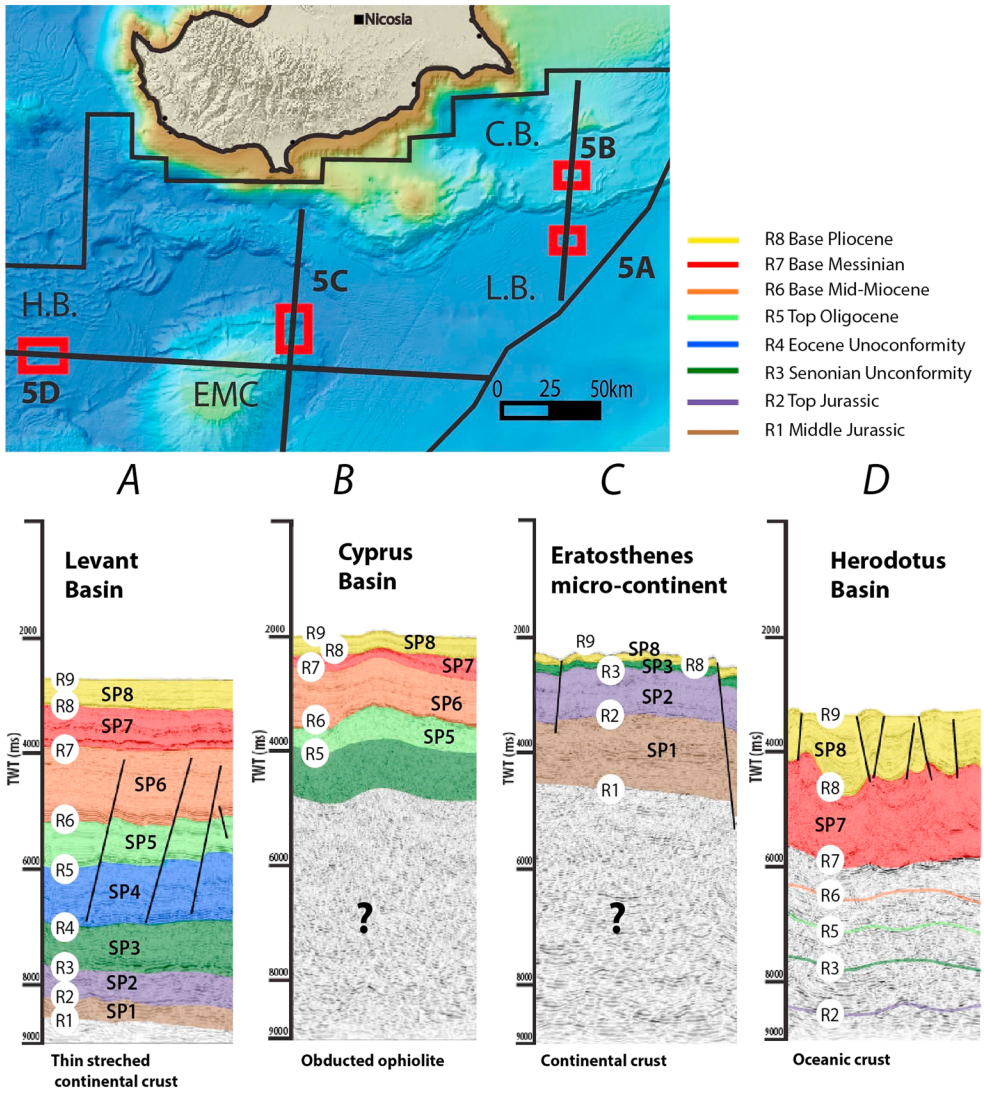

Figure 5. Stratigraphic columns illustrating the sedimentary filling of the four different domains, which are examined. The red boxes indicate the location of each column. Sequences as described in Figure 4. (a) Levant Basin domain: thick sedimentary infill above a thin stretched continental crust; (b) Cyprus Basin domain: thin sedimentary sequence, lacking in deposition of several seismic packages, perceived to be floored by obducted ophiolite; (c) Eratosthenes microcontinent domain: carbonate platform of Mesozoic age covered by Pliocene sediments, believed to be floored by continental crust; (D) Herodotus Basin domain: infilled by a very thick layer of Pliocene and Messinian deposits and floored by an oceanic crust. *Abbreviations:* L.B = Levant Basin, C.B = Cyprus Basin, E.S = Eratosthenes microcontinent, H.B = Herodotus Basin.

played an important role in the infilling of this basin as sediments of approximately 5 km thick were deposited, considerably less compared to the thickness of the Levant Basin sediments. The continuous uplift of this basin is also attested by the thin lenses of Messinian salt or the total absence of the salt in this domain.

The third domain is dominated by the Eratosthenes microcontinent (Figure 5c), south of Cyprus (Figure 5, box 5C). This is a carbonate platform constructed by carbonate buildups of Cretaceous and presumably Miocene age, overlain by a thin Pliocene cover ~100 m. Seismic interpretation of the Eratosthenes microcontinent suggests that the Eocene/Oligocene sediments are either absent or extremely thin. The basement of the Eratosthenes microcontinent is considered to be of thin continental crust (Welford et al., 2015).

The Herodotus basin is the fourth domain (Figure 5d) situated south-west of Cyprus (Figure 5, box 5D). It is filled by an estimated 14 km of sediments. Due to the lack of wells and data to tie the horizons, the older horizons are not identified. The thick Pliocene sediments (~2.5 km) and the very thick Messinian salt deposition

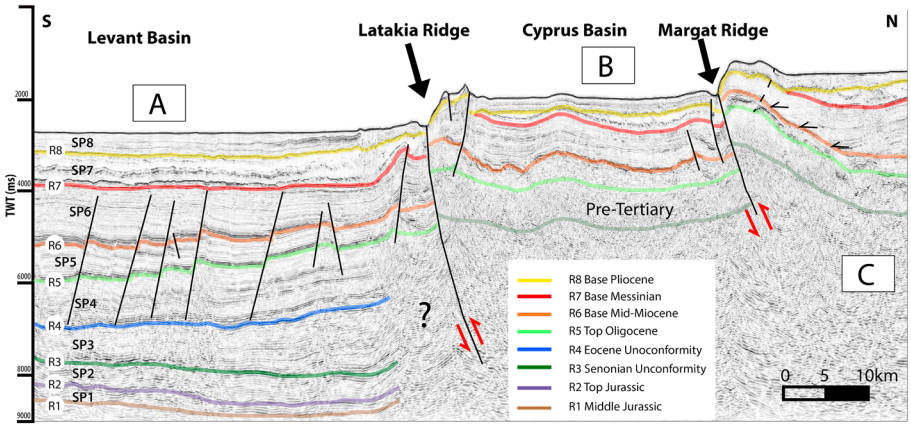

Figure 6. Seismic line 6063 trending south-north. The letters in squares are used to refer to a specific zone in the text. Position of this profile found in Figure 3. Position A: normal faults offsetting the early to middle Miocene sediments, commencing at the Eocene Unconformity horizon (R4) and dying out at the base of the Messinian horizon (R7). Position B: structurally higher position of the Cyprus Basin, infilled by a thin sedimentary sequence in comparison with the Levant Basin. Change in thickness of the Messinian salt between the Levant and Cyprus Basins implies the active nature of the Latakia Ridge. Position C: small basin of middle Miocene age as the early Miocene sediments are inclined toward the north with the mid-Miocene sediments onlapping on the slope of the basin.

(~2.5–3.8 km) are an indication of the continuous subsidence of the basin and the drastic infill from the Nile Delta. The challenges of subsalt imaging render it very difficult to identify any deep structures in this area.

4.2. Tectonic Structures and Timing of Deformation

A major subvertical fault described as the Latakia Ridge is identified on the seismic data and corresponds to a major boundary that separates the deeper Levant Basin to the south from the shallower Cyprus Basin to the north (i.e., the two first domains, presented above). This fault trends NE-SW to E-W and offsets the R7-Base Pliocene, R6-Base Messinian, R5-Base mid-Miocene, R4-Top Oligocene, and R2-Senonian unconformity horizons.

A comparison of the deposition of sediments north and south of the Latakia Ridge and from east to west is important in order to understand the spatial displacement of this structure. North and South of the Latakia Ridge, the thickness differentiation of the deposited sediments is more evident. South of the Latakia Ridge in the Levant Basin (Figure 6, position A), mid-Miocene deposits are ~1,600–1,800 m; the Messinian salt is ~1,500 m; and the Pliocene sediments are ~500–600 m. North of the Ridge, in the Cyprus Basin (Figure 6, position B), the mid-Miocene sediments are ~1,300–1,500 m, the Messinian salt is ~450 m, while the Pliocene deposits are ~400–500 m, indicative that the sedimentary sequence is thinner in the Cyprus Basin in comparison with the Levant Basin.

This thickness differentiation north and south of the Latakia Ridge provides evidence of the offset nature of the different seismic packages (SP), in particular SP6 (mid-Miocene ~1,400–1,600 m in the north compared to ~1,600–1,800 m in the south) and SP7 (Messinian ~450 m in the north and ~1,500 m in the south), an indication of the active thrusting nature of the Ridge from middle Miocene until Messinian time. The rather constant thickness of the SP8 package north and south of the Latakia Ridge provides difficulties in order to precisely determine the timing of the later deformation. However, it provides evidence of minor vertical movement since Pliocene time in the eastern area (Figure 6).

Comparing the Latakia Ridge from East to West, more information is collected in order to describe the lateral evolution of the Latakia Ridge. Just north of the Ridge, at the eastern extend of the Cyprus Basin, the mid-Miocene sediments (SP6) are ~1,300–1,500 m, the Messinian salt (SP7) is ~450 m, while the Pliocene deposits (SP8) are ~400–500 m (Figure 6, position B). In comparison in the western extend of the Cyprus Basin, deposition of mid-Miocene sediments (SP6) ranges from 500 to 800 m, Messinian salt (SP7) is restricted to ~250 m or it is not deposited, and the Pliocene sediments (SP8) are ~300–400 m (Figure 7, position D, Figure 8). Deposition of sequences SP6 and SP7 is observed to be thinning toward the west, indicative of the increasing vertical displacement along the Latakia Ridge and toward the west during mid-late Miocene

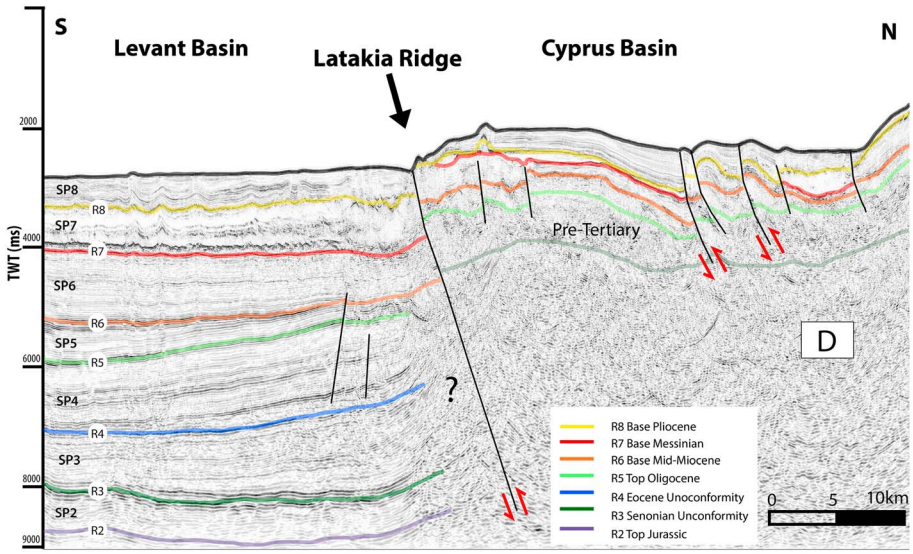

Figure 7. Seismic line 6061 trending south-north. The letter in square is used to refer to a specific zone in the text. Position of this profile found in Figure 3. Position D: piggyback basins created due to continuous convergence of the African plate with respect to the Eurasian plate.

time. For the depositions of SP8 in Pliocene time the thickness across the Latakia Ridge is rather constant. In the west (Figure 9), the SP8 is thicker in the Levant Basin in comparison with the Hecataeus Rise (Figure 3) situated north of the Latakia Ridge, which reflects an activity of Plio-Pleistocene time. This observation is in agreement with the pronounced bathymetric morphology associated with the Latakia Ridge. Notably, the relief observed on profile 6063 (Figure 6) is smaller than that on profile 6053 (Figure 9) marked by the Hecataeus Rise. This westward increase of vertical movement along the Latakia Ridge during Pliocene time is further attested by the deformation in the western domain of the Eratosthenes microcontinent. In the eastern domains, additional evidence for the active nature of the Ridge during Pliocene time is the transpressive flower structures identified north of the Latakia Ridge (Figure 6), which offset the SP6 and SP8 sediments.

Numerous extensional faults exist in the Levant Basin, which offset the Miocene and Oligocene sediments (Figure 6, position A). The offset of these normal faults is estimated to range between 150 and 450 m. The

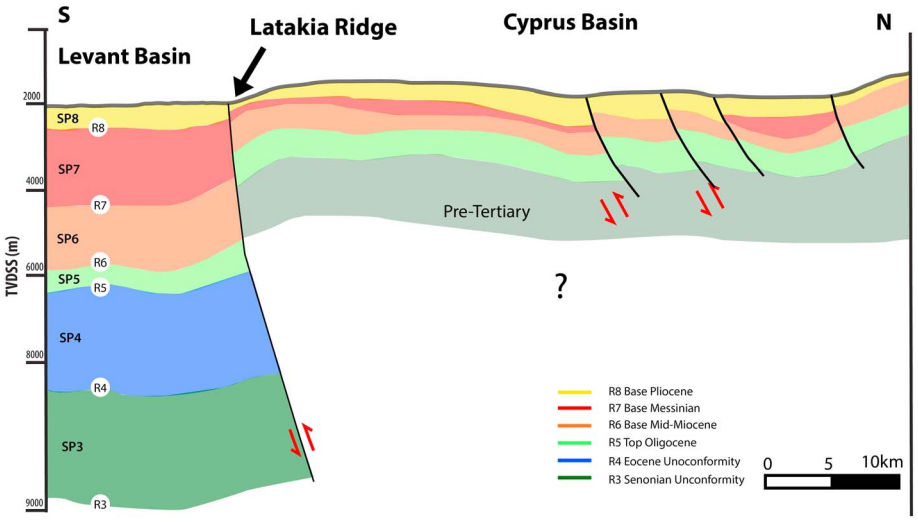

Figure 8. Schematic illustration of depth converted seismic reflectors, illustrating the depth converted packages as they were obtained by using the Dix formula and the stacked velocities.

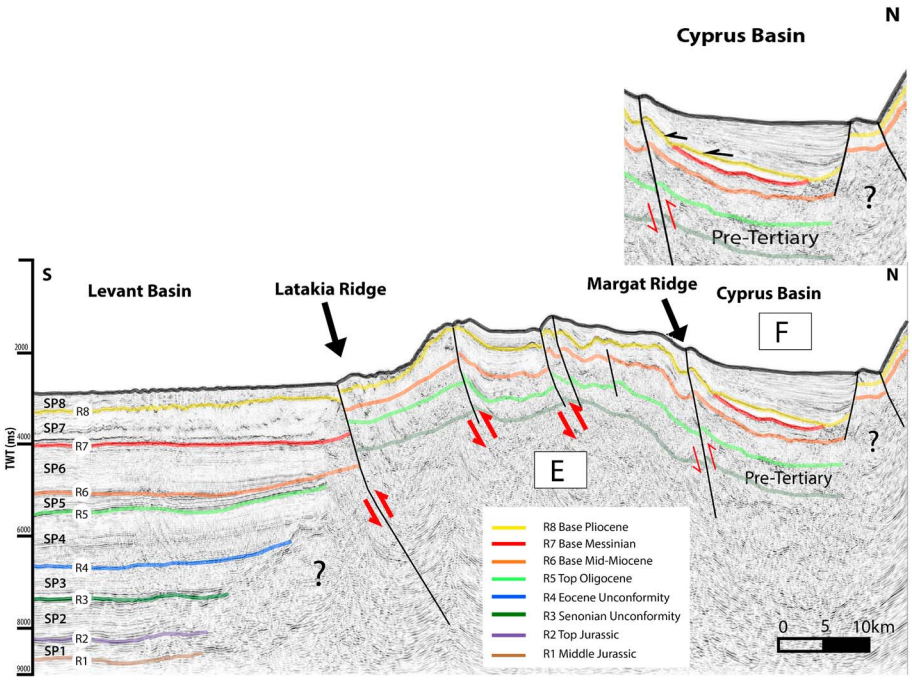

Figure 9. Seismic line 6053 trending south-north. The letter in square is used to refer to a specific zone in the text. Position of this profile found in Figure 3. Position E: thinning of the sedimentary sequence as we move toward the west, in comparison with the middle Miocene depositions of profile 6063. Position F: flexural basin created from the uplift of the Larnaca Ridge north of this seismic profile (as identified by Calon et al., 2005a). Inset is a zoomed image of the Cyprus Basin, illustrating thinning of the Pliocene sediments toward the south and onlaps on the Messinian and Miocene sediments.

majority of the faults are dipping toward the South, while occasionally, normal faults dipping to the north are observed. In positions where antithetic faults are observed, small horst structures are identified. The direction of the faults is E-W, although it is not well constrained from one profile to another, due to the sparse 2-D seismic data available (distance between lines ~20 and 30 km apart). These south dipping normal faults identified in the Levant Basin portray a deformation of middle to late Miocene age as they offset Oligocene-Miocene sediments and are confined in the R4 Eocene unconformity horizon at the base and the R7 Base Messinian horizon at the upper end.

The Cyprus Basin is an elongated structure that runs from east to west, with the Latakia and Larnaca Ridges constituting its southern and northern borders, respectively (Figure 3). It is in filled with sediments of Pre-Tertiary time (age undefined), SP5-early Miocene, SP6-middle/late Miocene, SP7-Messinian, and SP8-Pliocene/Pleistocene age. A regional unconformity marked by the R8 reflector is followed along all profiles and indicates a discontinuity in the deformation process. Folds in the Miocene units are sealed by the Pliocene package, indicating temporary interruption of the shortening. The convergence between the African and Eurasian plates results in the division of the Cyprus Basin into two smaller basins from the prominent Margat Ridge that trends almost E-W (Figure 6, position C). This structure is active during or in late early Miocene time, as evidenced by the thickness variations of SP5 in seismic profile 6063 (Figure 6, position C), where SP5 north of the Margat Ridge is thinner in contrast to the south of the Ridge.

In mid-Miocene, thickness variations are observed at the northern side of the Margat Ridge (Figure 6, position C) where the middle Miocene sediments are onlapping on northerly dipping early Miocene deposits. The thicker SP6 sequence south of the Ridge compared with the thinner SP6 deposition north of the Ridge (Figure 6, position C) indicates that the thrusting activity of the Margat Ridge during middle Miocene time. In late Miocene time the Margat Ridge was active, as it is displayed by the absence of the Messinian salt on the anticline north of the Margat Ridge (Figure 6, position C), while a salt body was deposited in the depression further north, which is directly linked with this thrusting activity. In line 6061 (Figure 7, position D) the

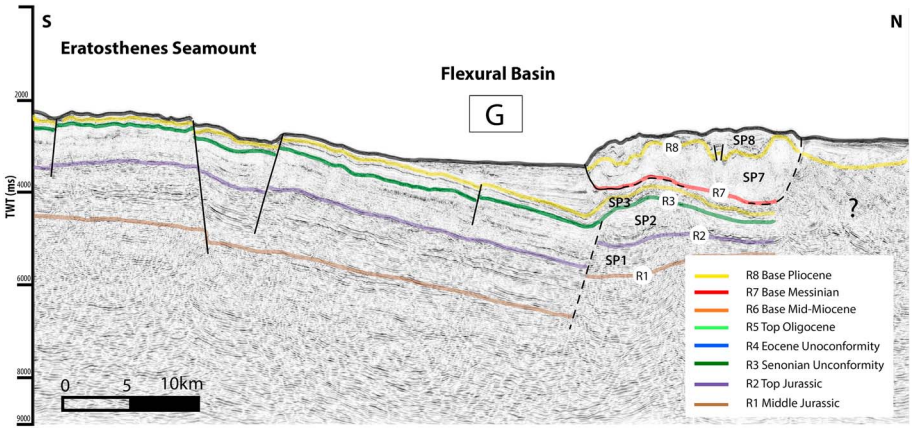

Figure 10. Seismic line 6015 trending south-north. The letter in square is used to refer to a specific zone in the text. Position of this profile found in Figure 3. Position G: flexural basin created from the convergence of Eratosthenes microcontinent with Cyprus and infilled by Plio-Pleistocene sediments. A thin skinned thrust with a décollement level north of the basin portrays the shortening.

piggyback basins express the active nature of the Ridge as the mid-Miocene strata are folded and the Messinian salt is not deposited.

Toward the west in-line 6053 (Figure 9), no substantial thickness differentiation of SP5 and SP6 is observed north and south of the Margat Ridge, which illustrates its limited or nonexistent activity during Early to middle Miocene time at this locality. The difference in depositional thickness of SP7 north and south of the Ridge points toward the renewed vertical movement along the Margat Ridge in Messinian time. Deformation during Pliocene to Recent time is identified through the seabed elevation. The higher bathymetric relief in the east (Figure 6, position C) compared to the west (Figure 8) may indicate that seismic line 6053 profile cuts the western tip of the Margat Ridge. Another feature illustrating Pliocene activity is the perceived transpressive flower structure observed north of the Margat Ridge (Figure 6, position B) offsetting SP6 and SP8 packages.

Although the Larnaca Ridge is observed only on a few of the available seismic lines for this study, evidence of its activity are observed from structures south of its position. A good example is seismic profile 6063 (Figure 6, position C) where the progressively thickening sequence of the middle Miocene sediments toward the north is connected with the thrusting activity of the Larnaca Ridge at this time.

During late Miocene time it is difficult to identify whether the Larnaca Ridge was active, as the Messinian salt deposition (Figure 6, position C) is of constant thickness and its continuation toward the north is not observed. In contrast, the active nature of the Larnaca Ridge during the Pliocene is illustrated in profile 6053 (Figure 9), where the seabed elevation changes abruptly in Pliocene time and a big flexural basin (Figure 9, position F) is created in filled by Plio-Pleistocene sediments of ~1,500 m. Detailed analysis of the flexural basin (Figure 9, inset image) illustrates the thrusting activity of the Larnaca Ridge in Pliocene time, as it is evident from the thinning Pliocene sediments toward the south and the onlaps depicted by the black arrows. These observations illustrate the synsedimentary thrusting activity of the Larnaca Ridge in Plio-Pleistocene time.

Further west in the Eratosthenes domain, thrusts and flexural basins are identified south and south-east of the Cyprus Island (Figure 10). On the northern dipping flank of the Eratosthenes microcontinent a flexural basin (Figure 10, position G) is observed in filled by Pliocene-Pleistocene sediments (~1,300 m), which are onlapping on the Cretaceous carbonate deposits. This flexural basin is a result of the thrusting of the Cyprus Arc (the arc is not observed on this profile, for position refer to inset image of Figure 11) due to the ongoing northward movement of the African plate and the collision of Eratosthenes microcontinent with Cyprus. The south verging thrust fault (Figure 10, position G) with a décollement level in the Messinian salt is indicative of shortening and could be the latest collision front between Eratosthenes microcontinent and Cyprus. The geometry of this thrust as it is observed on the seismic profile is connected with a pull-up effect due to the thick salt layer at this position and the big difference in velocities between the salt deposition of SP7 and the clastics of SP8.

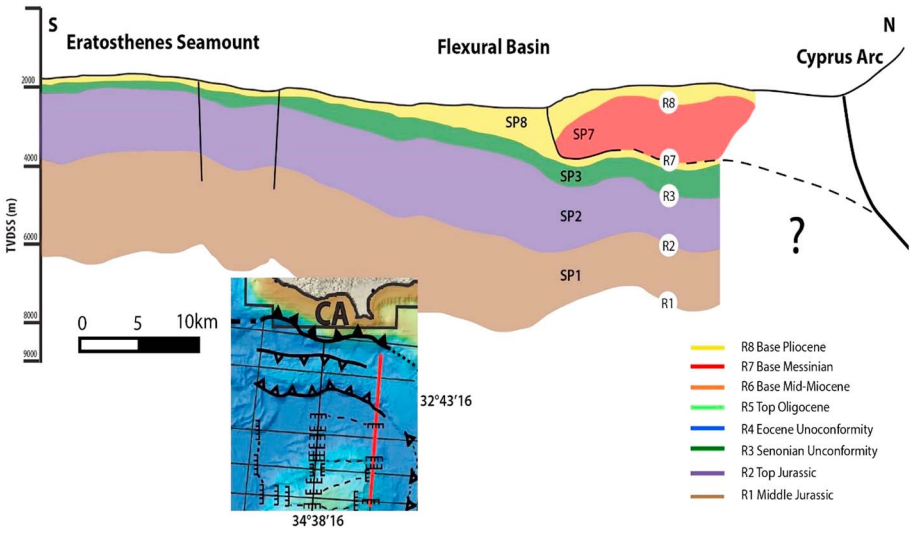

Figure 11. Schematic illustration of depth converted seismic reflectors that eliminate the large velocity contrast between SP8 (clastics) and SP7 (salt), which results in a pull-up effect as observed in Figure 10. SP3 is not steeply bending upward, and thus, a thrust fault is illustrated with a décollement level in the salt. The continuation toward the north is complex due to the limited and poor imaging. The seismic profile does not cross the Cyprus Arc, although the thrust fault (dashed line) is expected to connect with the Cyprus Arc. In-set bathymetry map with the location of the seismic profile displayed in red.

On the bathymetry map the geometry is indicative of salt advancement and salt flow, evidenced by the southward verging lobes (Figure 1) (e.g., Sigsbee escarpment; Hudec & Jackson, 2009). The salt is perceived as allochthonous as it rests on top of Pliocene sediments (Reiche & Hubsher, 2015). Similarly, the normal fault just below the salt that is illustrated with the dashed line in Figure 10 could be an inherited structure or it could be related to a pull-up effect as explained above.

A schematic illustration of depth converted seismic profiles is proposed (Figure 11), which portrays the elimination of the pull-up effect due to the big velocity contrast discussed above. By applying the standard Dix formula, a time to depth conversion model was built for each seismic horizon, by utilizing the stack velocities provided by PGS for every 2-D seismic profile. It is believed that the SP3 package (Figure 10) will not bend so steeply upward but will rather have a similar continuation as observed on the slope of Eratosthenes microcontinent. By accepting this scenario, the geometry of the fault becomes flat, with a décollement level in the salt, which could probably extend and connect at depth with the Cyprus Arc (Figures 3 and 10).

Several normal faults are identified on the crest of the Eratosthenes microcontinent (Figure 10). The main direction of these faults is E-W to WNW-ESE, and they offset Cretaceous and Pliocene sediments. The normal faults observed on the crest and northern flank of the Eratosthenes are of Pliocene age as they offset almost the whole sedimentary sequence. This feature could be associated with the flexure of the Eratosthenes microcontinent and the releasing of stress, due to the shortening that prevails in front of Eratosthenes as it collides with Cyprus.

5. Discussion

A variety of tectonic structures were identified and mapped offshore Cyprus. The main deformation mechanisms are related with thrust faults and later transpressive structures. As a result of the compressional regime flexural basins of various sizes are created. Other notable features are the array of normal faults described in the Levant Basin and on the Eratosthenes microcontinent. Fault activity is evident at least since early Miocene time and extends until the Present time, expressed through the continuous deformation identified along the Cyprus Arc system. The observed structures occur within a mosaic of juxtaposed domains, with each domain characterized by a distinctive crustal nature. Passing from east to west, these domains are (1) the Levant Basin domain, which is comprised by a thick sedimentary sequence of ~12 km and floored by a thin attenuated continental crust, (2) the Cyprus Basin domain infilled by a thin sequence of ~5 km of sediments

(Pre-Tertiary and Neogene age) and presumably underlain by obducted ophiolites, (3) the Eratosthenes microcontinent domain that constitutes a carbonate platform (~4 km) on top of a continental crust, and (4) the Herodotus Basin domain floored by an oceanic crust covered by a thick sedimentary sequence of ~14 km (Figure 1). Observations from the interpreted 2-D seismic profiles indicate that fault activity was more or less intense since early Miocene. Based on these results and by integrating data from previous onshore and offshore studies, a two-stage model of the deformation along the Cyprus Arc system from Neogene until Present time is proposed (Figure 12). This model takes into account the basic information observed from the seismic interpretation and illustrates the longitudinal change in deformation style along the Cyprus Arc system from East to West and through time.

5.1. Miocene

Deformation during Miocene is dominated by a compressive regime, which is expressed through a number of thrust faults. This thrusting activity results in the development of flexural basins and controls the geometry of the deposited sediments by shifting the positions of depocenters. Structures identified on the seismic profiles, such as the Latakia and Margat Ridges, illustrate a thrusting displacement at least since mid-Miocene time and until late Miocene as it is observed from the thickness variation of the sediments, north, and south of these structures (Figures 12a–12c).

Observations in this paper with regard to the deformation of the structures are in agreement with previous seismic reflection studies. Hall, Calon, et al. (2005) place the timing of uplift of the Latakia Ridge from mid-Miocene to late Miocene time as SP6 and SP7 are thickening toward the NNW. Similarly, Bowman (2011) connects the uplift of the Latakia Ridge with the deposition of a thinner sequence of SP6 and SP7 in the Cyprus Basin in comparison to the Levant Basin.

In order to counter data coverage limitations north of the Cyprus Basin, existing studies were taken in account. Calon et al. (2005b) identified that the Larnaca Ridge is uplifted in Middle to late Miocene time as the sediments are thick toward the north (away from the Ridge) but thin rapidly toward the Ridge. Mid-Miocene thrusting activity is also identified onshore in the Mesaoria Basin (Cleintuar et al., 1977; Harrison et al., 2008) as the Ovgos Fault zone is thrusting the deeper Kythrea flysch Formation next to the shallower pelagic marls and chalks of the Pakhna Formation (Cleintuar et al., 1977).

A new model is proposed regarding the thrusting activity of the structures and the propagation of deformation (Figures 12a–12c). A moderate activity is described for the Margat Ridge commencing in early Miocene time (Figure 12a). Although concrete evidence is missing from the available data for this study, moderate activity on the Larnaca Ridge is proposed in early Miocene time. A good indication of early Miocene activity of the Larnaca Ridge are the Oligo-Miocene highs identified onshore at the Cape Greco locality (eastern extend of Cyprus), which correspond to carbonate buildup s of the Terra Formation (Cleintuar et al., 1977). The prominent activity of the Margat Ridge is evident in mid-Miocene time with the onlapping mid-Miocene sediments on the inclined early Miocene sediments, while the southward Latakia Ridge is less active during this time (Figure 12b). Late Miocene activity on both structures is roughly equivalent (Figure 12c). All together these data indicate that thrusting activity migrates southward through time, thus following an in sequence development of the structures and a forward propagation of the deformation. The eventual end of this compressional event in Pliocene time resulted in a regional unconformity.

Continuous Neogene deformation along the Cyprus Arc system as it is described in this study commences in early Miocene time with an acme in late Miocene time can be correlated with the convergent regime between the Afro-Arabian and Eurasian plates. To the east, shortening in Syria is evidenced by the second phase of Syrian Arc folding, which initiated in early Miocene time in response to plate collision (Al Abdalla et al., 2010; Brew et al., 2001). In comparison to this prominent tectonic event in Syria, observations in this study indicate that deformation is limited in the west and more precisely on the Margat and Larnaca Ridges, while onshore Cyprus local uplift is suggested during the same time interval (Cleintuar et al., 1977). In conjunction with previous observations and evidence illustrated in this study, it is herein proposed that the westward attenuation of the deformation from Syria to Cyprus is related with the diversification of the crustal nature as in the vicinity of the Levant Basin continental crust and thin attenuated continental crust interact.

Despite the prominent compressional regime dictating the deformation style since the Late Cretaceous, normal faults of Oligo-Miocene age are identified in the Levant Basin. A clear deformation mechanism to

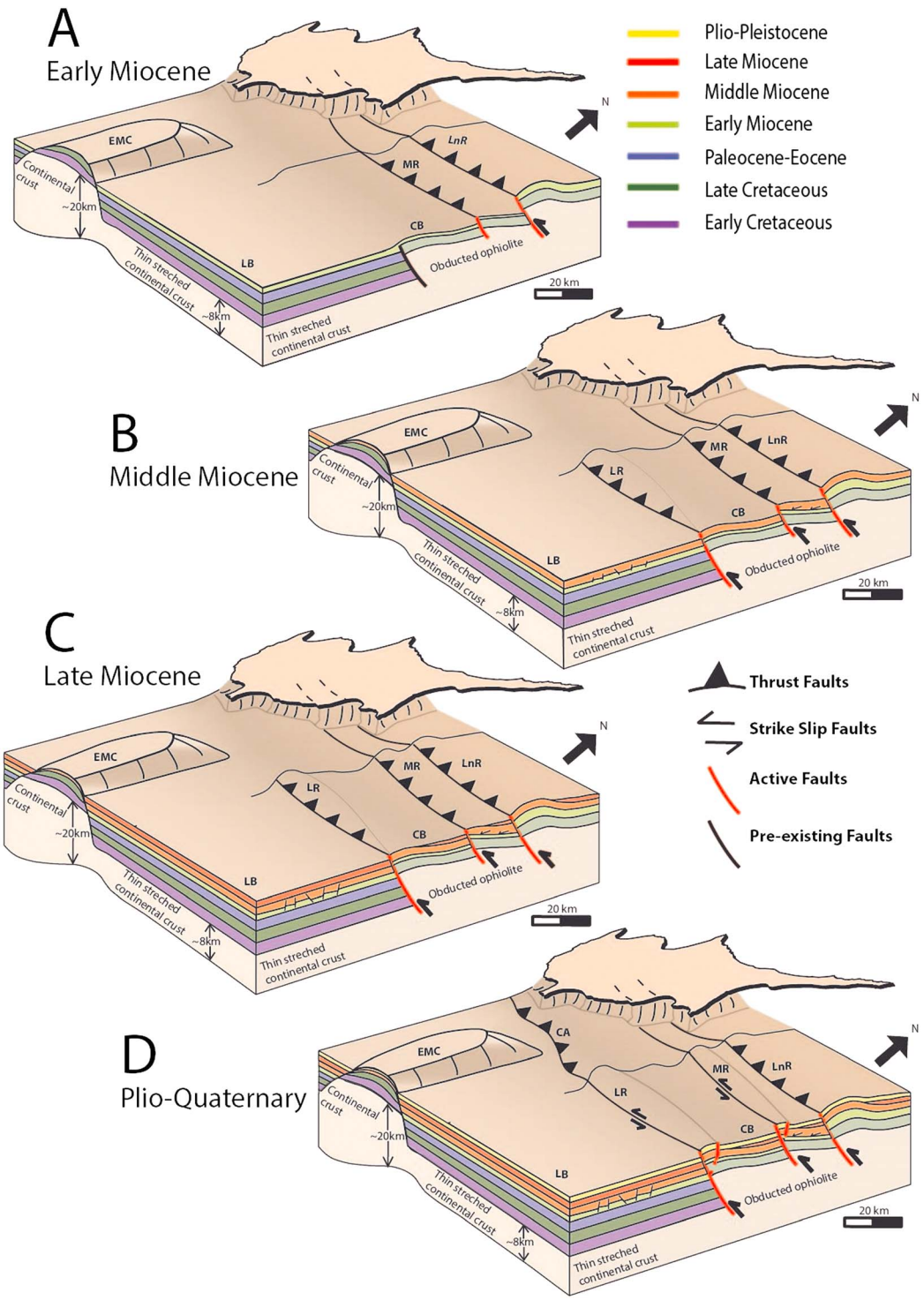

Figure 12. Tectonostratigraphic evolution offshore Cyprus in accordance with seismic interpretations in this paper and in connection with previous seismic studies from Calon et al. (2005a); Hall et al. (2005); Bowman (2011); Montadert et al. (2014). (a) Oligocene-early Miocene: The Larnaca and Margat Ridges are active as the early Miocene sediments are thinning north of the Margat Ridge, while the Latakia Ridge is covered by a thin sequence of early Miocene sediments. (b) Middle Miocene: Latakia and Margat Ridges are active, with mid-Miocene sediments onlapping on the inclined early Miocene sediments. Normal faults are initiating in the Levant Basin. (c) late Miocene: continuous activity of the Latakia, Margat, and Larnaca Ridges as Messinian salt is deposited into small depressions. Normal faults in the Levant Basin reach full growth restricted between the Eocene unconformity and base Messinian horizons. D: Pliocene-Recent: Active Latakia and Margat Ridges give rise to positive flower structures that indicate a transpressive strike-slip nature. Abbreviations as in Figure 3.

connect the compressional regime and the normal faults is difficult to envisage. Ghalayini et al. (2014, 2016) identified these NW-SE trending normal faults offshore Lebanon, suggesting that the faults are of nontectonic origin and are connected with the sedimentary nature of the Miocene deposits.

These normal faults are also identified on the seismic profiles (Figure 6a) that cover the Levant Basin offshore Cyprus (Figure 3). In this study, data limitations lead to a cautious approach as to the origin of these structures. Either the normal faults originate from nontectonic processes aided by the clay content in the host units, similar to what Ghalayini et al. (2014, 2016) proposed in Lebanon, or they are connected with the flexure of the upper crust and the creation of the normal faults in the sedimentary infill, in response to the continuous convergence of the African and Eurasian plates. These normal faults extend up to the late Miocene deposition of a thick layer of salt (~1.5–2 km) in the Levant Basin, which acts as the upper boundary that constrains the deformation in the Miocene deposits. The root of the normal faults terminates on the Eocene unconformity (horizon R4), and this could be related with the deposition of siliciclastic sediments that act as a barrier to the propagation of the deformation in older sediments. A solution for the origin of the normal faults could be attained through the interpretation of additional 2-D and 3-D data. This could provide the detailed direction of these structures, thus enabling the correlation of the faults with the prevailing tectonic regime.

5.2. Pliocene to Recent

Pliocene deformation along the Cyprus Arc evolved within a tectonic regime of thrust faulting and strike-slip structures, thus reflecting partitioning of deformation. This tectonic regime is described by a detailed description of transpressive flower structures, back thrusts, and more specifically by the comparison of the thickness of the Neogene sediments in the Cyprus Basin as they identified in this study, from observations across the Latakia and Margat Ridges (Figures 6 and 12d). Interpretations in this study illustrate that the Larnaca Ridge is reactivated by a thrusting mechanism with the creation of a Pliocene flexural basin in the footwall of the thrust (Figures 9f and 12d). These conclusions are in accordance with previous studies, which recognized positive flower structures along the Latakia and Margat Ridges (Bowman, 2011; Hall, Calon, et al., 2005) and further enhanced by the comparison of the thickness of the Neogene sediments as identified herein. In contrast, the Pliocene sediments that are thickening northward away from the Larnaca Ridge (Calon et al., 2005b), correlate well with the thrusting activity and the creation of the flexural basin described in this paper.

By combining the onshore and offshore data from previous publications and this research, it is evidenced herein that during the Pliocene, the tectonic regime at the plate boundary changes into a transpressive regime. This deformation style is connected with the fragmentation of the Eurasian continental plate and the westward expulsion of the Anatolian microplate, which is considered as the driving mechanism of the strike-slip motion. Deformation associated with the new tectonic regime was accommodated by the re activation of previous structures, such as the steeply vertical Latakia Ridge, which is located at a preexisting zone of weakness that separates different crustal domains (Levant and Cyprus Basins).

As identified by the interpretation of different seismic profiles in this study, the longitudinal evolution of deformation along the Cyprus Arc system changes along strike. In the eastern domain the Latakia Ridge is mainly described by strike-slip motion, whereas in the western domain, directly south of Cyprus, a thrusting regime is evidenced from the creation of a big flexural basin (Figures 10f and 12d). This shortening is connected with the collision of the Eratosthenes microcontinent with Cyprus, and it is considered as the most intense phase of uplift on Cyprus (Harrison et al., 2012; Kinnaird & Robertson, 2012). The intense uplift at that period is also supported inland, by the change in sedimentation, with the deposition of carbonates ceasing (chalks and marls of Pakhna Formation) and the deposition of clastics initiating in early Pliocene (sandstones and biocalcarenites of Nicosia Formation). The Mesozoic structuration of the Levant Basin, which juxtaposed different crustal blocks, is therefore regarded as a major cause for the east-west evolution of the deformation along the plate structures of the Cyprus Arc.

6. Conclusions

Based on the interpretation of the 24 regional 2-D reflection seismic profiles traversing the Cyprus Arc system and the regional structural settings, the following conclusions can be drawn:

1. Mapped tectonic structures with a pronounced bathymetric expression include thrust faults and strike-slip faults active from Miocene to Present and the creation of flexural basins of the same age. A number of layer bound normal faults were recognized within the Eocene-Miocene package.
2. Generally, shortening dominated during the interpreted Neogene time interval, whereas strain partitioning, with both thrusting and strike-slip movements, characterizes the Plio-Pleistocene deformations as the result of the westward movement of Anatolia.
3. The temporal and longitudinal evolution of the deformation style along the investigated Cyprus Arc system is a consequence of the composite nature of the eastern Mediterranean crust and the individualization of the Anatolia microplate.
4. The documented Plio-Pleistocene tectonic structures (positive flower structures in the east and flexural basin in the west) suggest a westward increase of shortening, in relation with the lateral change in nature of the crust, passing from a thinned continental crust in the Levant Basin (eastern domain) to the continental crust that underlays the Eratosthenes microcontinent domain.

Acknowledgments
AcknowledgementThe first author would like to acknowledge the Cypriot Ministry of Energy, Commerce, Industry, and Tourism for funding this project. Petroleum Geo-Services (PGS) is acknowledged for providing the seismic data. A very warm thank you to Jean Letouzey for his insights and the constructive discussions on the geological structures in the eastern Mediterranean. Dominique Frizon de Lamotte, an Associate Editor, an anonymous reviewer, and Editor John Geissman are thanked for their valuable reviews, which aided in improving this manuscript. Data presented in this study could be accessed at https://www.pgs.com/data-library/europe/mediterranean/ by contacting PGS.

References

Aksu, A. E., Hall, J., & Yaltirak, C. (2005). Miocene to Recent tectonic evolution of the eastern Mediterranean: New pieces of the old Mediterranean puzzle. *Marine Geology*, *221*, 1–13.

Al Abdalla, A., Barrier, E., Matar, A., & Muller, C. (2010). Late Cretaceous to Cenozoic tectonic evolution of the NW Arabian platform in NW Syria. In C. Homberg & M. Bachmann (Eds.), *Evolution of the Levant Margin and Western Arabia Platform Since the Mesozoic*, *Geological Society, London, Special Publications* (Vol. 341, pp. 305–327).

Barrier, E., & Vrielynch, B. (2008). Paleotectonic maps of the Middle East: Tectono sedimentary palinspastic maps from Late Norian to Pliocene, 14 maps, Comm. la Cart. Geol. du monde

Ben-Avraham, Z., Ginzburg, A., Makris, J., & Eppelbaum, L. (2002). Crustal structure of the Levant basin, Eastern Mediterranean. *Tectonophysics*, *346*, 23–43.

Bowman, S. (2011). Regional seismic interpretation of the hydrocarbon prospectivity of offshore Syria. *GeoArabia*, *16*, 95–124.

Brew, G., Barazangi, M., Al-Maleh, A. K., & Sawaf, T. (2001). Tectonic and geological evolution of Syria. *GeoArabia*, *6*(4), 573–616.

Calon, T. J., Aksu, A. E., & Hall, J. (2005a). The Neogene evolution of the Outer Latakia Basin and its extension into the Eastern Mesaoria Basin (Cyprus), Eastern Mediterranean. *Marine Geology*, *221*, 61–94.

Calon, T. J., Aksu, A. E., & Hall, J. (2005b). The Oligocene-Recent evolution of the Mesaoria Basin (Cyprus) and its western marine extension, Eastern Mediterranean. *Marine Geology*, *221*, 95–120.

Cleintuar, M. R., Knox, G. J., & Ealey, P. J. (1977). The geology of Cyprus and its place in the East-Mediterranean framework. *Geologie en Mijnbouw*, *56*, 66–82.

Dilek, Y., & Altunkaynak, S. (2009). Geochemical and temporal evolution of Cenozoic magmatism in western Turkey: Mantle response to collision, slab break-off and lithospheric tearing. In D. J. J. van Hinsbergen, M. A. Edwards, & R. Govers (Eds.), *Collision and Collapse at the Africa-Arabia-Eurasia Subduction Zone*, *Geological Society, London, Special Publications* (Vol. 311, pp. 213–233).

Dilek, Y., & Sandvol, E. (2009). Seismic structure, crustal architecture and tectonic evolution of the Anatolian–African plate boundary and the Cenozoic orogenic belts in the Eastern Mediterranean Region. In J. B. Murphy, J. D. Keppie, & A. J. Hynes (Eds.), *Ancient Orogens and Modern Analogues*, *Geological Society, London, Special Publications* (Vol. 327, pp. 127–160).

Faccenna, C., Bellier, O., Martinod, J., Piromallo, C., & Regard, V. (2006). Slab detachment beneath eastern Anatolia: A possible cause for the formation of the North Anatolian fault. *Earth and Planetary Science letters*, *242*, 85–97.

Frizon de Lamotte, D., Raulin, C., Mouchot, N., Wrobel-Daveau, J.-C., Blanpied, C., & Ringenbach, J.-C. (2011). The southernmost margin of the Tethys realm during the Mesozoic and Cenozoic: Initial geometry and timing of the inversion processes. *Tectonics*, *30*, TC3002. https://doi.org/10.1029/2010TC002691

Gardosh, M., & Druckman, Y. (2006). Seismic stratigraphy, structure and tectonic evolution of the Levantine basin, offshore Israel. In A. H. F. Robertson & D. Mountrakis (Eds.), *Tectonic Development of the Eastern Mediterranean Region*, *Geological Society, London, Special Publications* (Vol. 260, pp. 201–227).

Gardosh, M., Garfunkel, Z., Druckman, Y., & Buchbinder, B. (2010). Tethyan rifting in the Levant region and its role in early Mesozoic crustal evolution. In C. Homberg & M. Bachmann (Eds.), *Evolution of the Levant Margin and Western Arabia Platform Since the Mesozoic*, *Geological Society, London, Special Publications* (Vol. 341, pp. 9–36).

Garfunkel, Z. (1998). Constrains on the origin and the history of the Eastern Mediterranean basin. *Tectonophysics*, *298*, 5–35.

Garfunkel, Z. (2004). Origin of the Eastern Mediterranean basin: A re-evaluation. *Tectonophysics*, *391*, 11–34.

Ghalayini, R., Daniel, J. M., Homberg, C., & Nader, F. H. (2016). Growth of layer-bound normal faults under a regional anisotropic stress field. In C. Childs, et al. (Eds.), *The Geometry and Growth of Normal Faults*, *Geological Society, London, Special Publications* (Vol. 439, pp. 57–78).

Ghalayini, R., Daniel, J. M., Homberg, C., Nader, F. H., & Comstock, J. E. (2014). Impact on Cenozoic strike-slip tectonics on the evolution of the northern Levant Basin (offshore Lebanon). *Tectonics*, *33*. https://doi.org/10.1002/2014TC003574

Ghalayini, R., Daniel, J. M., Homberg, C., Nader, F. H., Darnault, R., Mengus, J. M., & Barrier, E. (2017). The effect of the Palmyra Trough and Mesozoic structures on the Levant margin and on the evolution of the Levant restraining bend. In F. Roure, et al. (Eds.), *Lithosphere Dynamics and Sedimentary Basins of the Arabian Plate and Surrounding Areas, Frontiers in Earth Sciences* (pp. 149–172). https://doi.org/10.1007/978-3-319-44726-1_7

Granot, R. (2016). Palaeozoic oceanic crust preserved beneath the eastern Mediterranean. *Nature Geoscience*, *9*, 701–705.

Hall, J., Aksu, A. E., Calon, T. J., & Yasar, D. (2005). Varying tectonic control on basin development at an active microplate margin: Latakia basin, eastern Mediterranean. *Marine Geology*, *221*, 15–60.

Hall, J., Calon, T. J., Aksu, A. E., & Meade, S. R. (2005). Structural evolution of the Latakia Ridge and Cyprus basin at front of the Cyprus Arc, Eastern Mediterranean sea. *Marine Geology*, *221*, 261–297.

Harrison, R. W. (2008). A model for the plate tectonic evolution of the Eastern Mediterranean region that emphasizes the role of transform (strike-slip) structures. In *1st WSEAS International conference on Environmental and Geological Science and Engineering (EG'08) Malta*, *September 11–13*, *2008*.

Harrison, R. W., Newell, W., Panayides, I., Stone, B., Tsiolakis, E., Necdet, M., …, Schindler, S. J. (2008). Bedrock geological map of the greater Lefkosia Area, Cyprus. In *US Geological Survey Scientific Investigations Map*, *3046*.

Harrison, R. W., Tsiolakis, E., Stone, B. D., Lord, A., McGeehin, J. P., Mahan, S. A., & Chirico, P. (2012). Late Pleistocene and Holocene uplift history of Cyprus: Implications for active tectonics along the southern margin of the Anatolian microplate. *Geological Society, London, Special Publications*, *372*, 561–584.

Hawie, N., Gorini, C., Deschamps, R., Nader, F. H., Montadert, L., Granjeon, D., & Baudin, F. (2013). Tectono-stratigraphic evolution of the northern Levant Basin (offshore Lebanon). *Marine and Petroleum Geology*, *48*, 392–410.

Homberg, C., Barrier, E., Mroueh, M., Muller, C., Hamdan, W., & Hizagi, F. (2010). Tectonic evolution of the central Levant domain (Lebanon) since Mesozoic time. In C. Homberg & M. Bachmann (Eds.), *Evolution of the Levant Margin and Western Arabia Platform Since the Mesozoic*, *Geological Society, London, Special Publications* (Vol. 341, pp. 245–268).

Hsu, K. J., Montadert, L., Bernoulli, D., Cita, M. B., Erickson, A., Garrison, R. E., … Wright, R. (1977). History of the Mediterranean salinity crisis. *Nature*, *267*, 399–403.

Hudec, M. R., & Jackson, M. P. A. (2009). Interaction between spreading salt canopies and their peripheral thrust systems. *Journal of Structural Geology*, *31*, 1114–1129.

Inati, L., Zeyen, H., Nader, F. H., Adelinet, M., Sursock, A., Rahhal, M. E., & Roure, F. (2016). Lithospheric architecture of the Levant Basin (Eastern Mediterranean region): A 2D modeling approach. *Tectonophysics*, *693*, 143–156.

Kempler, D. (1998). Eratosthenes Seamount: The possible spearhead of incipient continental collision in the Eastern Mediterranean. In A. H. F. Robertson, et al. (Eds.), *Proceedings of the Ocean Drilling Program*, *Scientific Results* (Vol. 160, pp. 709–721). College Station, TX.

Kempler, D., & Garfunkel, Z. (1994). Structures and kinematics in the northeastern Mediterranean: A study of an irregular plate boundary. *Tectonophysics*, *234*, 19–32.

Kinnaird, T. C., & Robertson, A. H. F. (2012). Tectonic and sedimentary response to subduction and incipient continental collision in southern Cyprus, easternmost Mediterranean region. *Geological Society, London, Special Publications*, *373*, 585–614.

Kinnaird, T. C., Robertson, A. H. F., & Morris, A. (2011). Time of uplift of the Troodos massif (Cyprus) constrained by sedimentary and magnetic polarity evidence. *Journal of the Geological Society*, *168*, 457–470.

Klimke, J., & Ehrhardt, A. (2014). Impact and implication of the Afro-Eurasian collision south of Cyprus from reflection seismic data. *Tectonophysics*, *626*, 105–119.

Le Pichon, X., & Kreemer, C. (2010). The Miocene-to-Present kinematic evolution of the Eastern Mediterranean and Middle East and its implications for Dynamics. *Annual Review of Earth and Planetary Sciences*, *2010*, 323–351.

Makris, J., Ben-Avraham, Z., Behle, A., Ginzburg, A., Giese, P., Steinmetz, L., … Eleftheriou, S. (1983). Seismic refraction profiles between Cyprus and Israel and their interpretation. *Geophysical Journal of the Royal Astronomical Society*, *75*, 575–591.

McClusky, S., Balassanian, S., Barka, A., Demir, C., Ergintav, S., Georgiev, I., … Veis, G. (2000). Global Positioning System constraints on plate kinematics and dynamics in the eastern Mediterranean and Caucasus. *Journal of Geophysical Research*, *105*, 5695–5719.

McClusky, S., Reilinger, R., Mahmoud, S., Ben Sari, D., & Tealeb, A. (2003). GPS constraints on Africa (Nubia) and Arabia plate motions. *Geophysical Journal International*, *155*, 126–138.

Montadert, L., Lie, O., Semb, P. H., & Kassinis, S. (2010). New seismic may put offshore Cyprus hydrocarbon prospects in the spotlight. *First Break*, *28*, 91-101.

Montadert, L., Nicolaides, S., Semb, H. P., & Lie, O. (2014). Petroleum systems offshore Cyprus. In L. Marlow, C. Kendall, & L. Yose (Eds.), *Petroleum Systems of the Tethyan Region*, *AAPG memoir 106* (pp. 301–334).

Netzeband, G., Gohl, K., Hubscher, C., Ben-Avraham, Z., Dehghani, G., Gajewski, D., & Liersch, P. (2006). The Levantine basin—Crustal structure and origin. *Tectonophysics*, *418*, 167–188.

Reiche, S., & Hubscher, C. (2015). The Hecataeus Rise, easternmost Mediterranean: A structural record of Miocene-Quaternary convergence and incipient continent continent collision at the African-Anatolian plate boundary. *Marine and Petroleum Geology*, *67*, 368–388.

Reilinger, R., McClusky, S., Vernant, P., Lawrence, S., Ergintav, S., Cakmak, R., … Karam, G. (2006). GPS constraints on continental deformation in the Africa-Arabia-Eurasia continental collision zone and implications for the dynamics of plate interactions. *Journal of Geophysical Research*, *111*, B05411. https://doi.org/10.1029/2005JB004051

Ricou, L. E. (1971). Le croissant péri-arabe: Une ceinture de nappes mises en place au Crétacé supérieur. *Revue de Géographie Physique et de Géologie Dynamique*, *13*, 327–350.

Roberts, G., & Peace, D. (2007). Hydrocarbon plays and prospectivity of the Levantine basin, offshore Lebanon and Syria from modern seismic data. *GeoArabia*, *12*, 99–124.

Robertson, A. H. F. (1998). Tectonic significance of the Eratosthenes Seamount: A continental fragment in the process of collision with a subduction zone in the eastern Mediterranean (Ocean Drilling Program Leg 160). *Tectonophysics*, *298*, 63–82.

Robertson, A. H. F. (2007). Overview of tectonic settings related to the rifting and the opening of Mesozoic ocean basins in the Eastern Tethys: Oman, Himalayas and Eastern Mediterranean regions. In G. D. Kamer, G. Manatschal, & L. M. Pinheiro (Eds.), *Imaging, Mapping and Modeling Continental Lithosphere Extension and Breakup*, *Geological Society, London, Special Publications* (Vol. 282, pp. 325–388).

Robertson, A. H. F., Parlak, O., & Ustaomer, T. (2012). Overview of the Paleozoic-Neogene evolution of the Neotethys in the Eastern Mediterranean region (southern Turkey, Cyprus, Syria). *Petroleum Geoscience*, *18*, 381–404.

Sage, L., & Letouzey, J. (1990). Convergence of the African and Eurasian Plate in the Eastern Mediterranean. In J. Letouzey & Editions Technip (Eds.), *Petroleum and Tectonics in Mobile Belts* (pp. 49–68). Paris.

Segev, A., Schattner, U., & Lyakhovsky, V. (2011). Middle-Late Eocene structure of the southern Levant continental margin—Tectonic motion versus global sea-level change. *Tectonophysics*, *499*, 165–177.

Stampfli, G. M., & Borel, G. D. (2002). A plate tectonic model for the Paleozoic and Mesozoic constrained by dynamic plate boundaries and restored synthetic oceanic isochrones. *Earth and Planetary Science Letters*, *196*, 17–33.

Vidal, N., Alvarez-Marron, J., & Klaeschen, D. (2000). The structure of the Africa-Anatolia plate boundary in the eastern Mediterranean. *Tectonics*, *19*(4), 723–739.

Vidal, N., Klaeschen, D., Kopf, A., Docherty, C., Von Huene, R., & Krasheninnikov, V. A. (2000). Seismic images at the convergence zone from south of Cyprus to the Syrian coast, eastern Mediterranean. *Tectonophysics*, *329*, 157–170.

Welford, J. K., Hall, J., Hubscher, C., Reiche, S., & Louden, K. (2015). Crustal seismic velocity structure from the Eratosthenes Seamount to Hecataeus Rise across the Cyprus Arc, eastern Mediterranean. *Geophysical Journal International*, *200*, 933–951.